

Damping behaviour of dynamically cured butyl rubber/polypropylene blends

Fu-Sen Liao

New Materials Research and Development, China Steel Corporation, Kaohsiung, Taiwan 81233, Republic of China

and An-Chung Su* and Tzu-Chien J. Hsu

Institute of Materials Science and Engineering, National Sun Yat-Sen University, Kaohsiung, Taiwan 80424, Republic of China
(Received 29 March 1993; revised 2 August 1993)

Dynamically cured blends of butyl rubber (IIR; isoprene–isobutylene rubber) and anhydride-grafted polypropylene (PP) of various component ratios and curative loadings were prepared by melt mixing. Evidence from dynamic mechanical analysis and phase-contrast microscopy suggested that these blends were heterogeneous, with the PP phase being continuous. Damping characteristics of these blends in the temperature range of -60 to 0°C were strongly affected by a liquid-state relaxation peak of the IIR phase. It was observed that the presence of a continuous PP phase tends to suppress the intensity of this characteristic loss peak and shift it towards lower temperatures; on the other hand, the crosslinking of IIR has little effect on the intensity of the broad loss peak but tends to shift it towards higher temperatures. These observations were interpreted in terms of effects of thermal misfit stress and crosslinking on the liquid–liquid transition of the IIR phase.

(Keywords: mechanical damping; dynamically vulcanized blends; butyl rubber/polypropylene)

INTRODUCTION

Butyl rubber (IIR), a copolymer of isoprene (typically 1–5%) and isobutylene, is well known for its high energy absorptivity¹. IIR and its halogenated derivatives can be vulcanized by use of conventional sulfur curatives or phenol–formaldehyde resins (resoles)^{2,3}. Capps *et al.*^{4,5} indicated that the dynamic mechanical properties of chlorinated IIR (vulcanized using several cure systems) are influenced by the extent of crosslinking, the type of curative and the filler loading. Dutta and Tripathy⁶ showed clearly that the dynamic mechanical properties (and ageing characteristics) of brominated IIR depend significantly on the concentration of a phenolic curative.

Comprising cured rubber domains dispersed in a thermoplastic matrix, dynamically vulcanized rubber/plastic blends possess many of the properties of the cured rubber while retaining the thermoplastic-like processibility^{7–11}. The general properties of dynamically cured butyl rubber/polypropylene (IIR/PP) blends have been previously documented¹². In a preliminary study¹³, we have shown that dynamically cured IIR/PP blends can be used with reasonable success for the purpose of vibration damping in the constrained-layer configuration. In this configuration, the damping characteristics of the laminate are governed¹⁴ by the dynamic mechanical properties of the viscoelastic layer, especially the loss tangent ($\tan \delta$) in the glass transition (T_g) region. However, the dynamic mechanical behaviour of dynamically cured

IIR/PP blends has not been systematically investigated in the literature.

In this study, dynamically cured IIR/PP blends of various compositions and curative levels were prepared. The dynamic mechanical properties of these blends and, for comparison purposes, the corresponding IIR vulcanizates were examined and discussed.

EXPERIMENTAL

Materials

The IIR material was Butyl 301 from Polysar, with an unsaturation of 1.7 mol%. The PP material (Admer QE-050 from Mitsui Petrochemical) was lightly (ca. 1%) anhydride-modified. The curative was a brominated phenolic resin (SP-1056 from Schenectady Chemicals) with a melting point of 61°C .

Sample preparation

Compounding and blending. A laboratory-scale internal mixer (Plasti-corder PL2000, Brabender) equipped with a pair of roller blades was used for both compounding and blending purposes. Compounds of IIR with different curative levels (0 to 10 phr) were prepared via mechanical mixing at 80°C for 5 min under a rotor rate of 40 rpm. In the subsequent mechanical blending process, the rotor rate was kept at 40 rpm and the mixing temperature was set at 180°C . The PP material was fed first into the preheated mixing chamber; the IIR compound was added 1 min later. The dynamical curing was allowed to proceed

* To whom correspondence should be addressed

for 9 min after loading of IIR. A blank PP sample without the addition of IIR compound was prepared in a similar manner.

Compression moulding. The dynamically cured blends and the PP blank were compression moulded (20 min at 200°C) in a Carver press (equipped with water-cooling accessories) to form sheets ca. 3 mm in thickness. The moulded sheets were slowly cooled within the mould to room temperature in a consistent manner such that sample-to-sample differences in thermal history were considered insignificant.

For comparison purposes, statically cured IIR vulcanizates were also prepared. The IIR compounds were first compression moulded at 180°C for 10 min; the mould temperature was then raised to 200°C at 5°C min⁻¹ and maintained at 200°C for an additional 10 min before cooling to room temperature. The composition and the cure process for the moulded samples are summarized in Table 1.

Characterization

Optical microscopy. Morphological observations were made over thin sections (ca. 0.2 µm thick, ultramicrotomed at ca. -120°C) of blends using an optical microscope (Optiphot-Pol, Nikon) equipped with a phase contrast unit (PH-21N, Nikon).

Differential scanning calorimetry. Melting behaviour of the as-moulded blends and the PP blank was examined by means of differential scanning calorimetry (d.s.c.) using a Perkin-Elmer DSC7 instrument at a heating rate of 10°C min⁻¹. The crystallinity of the PP phase was calculated from the measured heat of fusion and the reported estimate¹⁵ for the heat of fusion (209 J g⁻¹) of perfectly crystalline PP.

Dynamic mechanical analysis. Dynamic mechanical measurements were made over rectangular bars (cut from the compression-moulded sheets) using a dynamic rheological spectrometer (RDS-II, Rheometrics) operated in the torsion mode at a frequency of 1 Hz and a heating rate of 3°C min⁻¹. Unless specified otherwise, a maximum strain of 0.05% was typically adopted.

Gel fraction determination. Soxhlet extraction (in xylene) was used to determine the gel content (ϕ_{gel}) in the vulcanized IIR phase. Specimens of IIR vulcanizates or IIR/PP blends ca. 1.0 g in weight were cut into thin slices and extracted for 8 h. After extraction, the swollen gel was vacuum-dried overnight at 100°C before weighing. The weight fraction of the residual gel, normalized with respect to the initial rubber content, was taken as ϕ_{gel} . A subsequent d.s.c. analysis showed the presence of only insignificant amounts of PP in the insolubles, confirming Coran's earlier observation⁸ that PP was essentially completely extractable from the dynamically vulcanized blends with boiling xylene.

Measurement of crosslinking density. The crosslinking density in the IIR phase was determined by means of equilibrium swelling using the Flory-Rehner equation¹⁶:

$$\nu = -[\ln(1 - \phi_r) + \phi_r + \chi\phi_r^2]/2[V_s(\phi_r^{1/3} - \phi_r/2)] \quad (1)$$

where ν is the number of effective network chains per unit volume of rubber, ϕ_r the volume fraction of rubber

Table 1 Designation of samples

Sample code	Composition (wt%)		Amount of curative in the IIR compound (phr)	Vulcanization process
	PP	IIR compound		
I-0	0	100	0	Static
I-0	0	100	2.5	Static
I-3	0	100	7.5	Static
I-4	0	100	10	Static
B5.0	50	50	0	Dynamic
B5-1	50	50	2.5	Dynamic
B5-2	50	50	5	Dynamic
B5-3	50	50	7.5	Dynamic
B5-4	50	50	10	Dynamic
B3-4	70	30	10	Dynamic
B4-4	60	40	10	Dynamic
B6-4	40	60	10	Dynamic
B7-4	30	70	10	Dynamic

Table 2 Characteristics of statically vulcanized IIR at different curative levels^a

Sample code	ϕ_{gel}^b	ν_{bulk}^c (mol m ⁻³)	ν_{gel}^d (mol m ⁻³)	$\nu_{\text{bulk,calc}}^e$ (mol m ⁻³)
I-1	0.87	10	16	14
I-3	0.89	13	14	12
I-4	0.90	15	16	14

^a Cf. Table 1 for sample designations

^b Soxhlet extraction in boiling xylene

^c Equilibrium swelling of the as-moulded specimen in cyclohexane at room temperature

^d Equilibrium swelling of the xylene-insolubles in cyclohexane at room temperature

^e Calculated according to equation (2)

in the swollen network, V_s the molar volume of the solvent, and χ the polymer-solvent interaction parameter. The swelling measurements were performed at room temperature using cyclohexane as the solvent. After reaching equilibrium swelling (which took typically a month), the swollen specimens were weighed, vacuum-dried overnight at 80°C and weighed again to determine ϕ_r . The value of χ was taken¹⁷ as 0.433 for the IIR/cyclohexane pair.

For IIR vulcanizates, specimens were cut directly from the as-formed sheets; therefore, the swelling measurements gave directly the bulk crosslinking density (ν_{bulk}). In the case of IIR/PP blends, dried gels after Soxhlet extraction were used; the measured crosslinking density (ν_{gel}) corresponded to the gel. The bulk crosslinking density in the original IIR phase of the blend was then estimated according to:

$$\nu_{\text{bulk}} = \nu_{\text{gel}}\phi_{\text{gel}} \quad (2)$$

The validity of this procedure was tested by performing swelling experiments on xylene-extracted IIR vulcanizates. As shown in Table 2, results from the two approaches are in reasonable agreement.

RESULTS AND DISCUSSION

Morphological features

Representative morphological features of the present blends are shown in Figure 1. The unvulcanized B5-0 blend (Figure 1a) is characterized by a two-phase

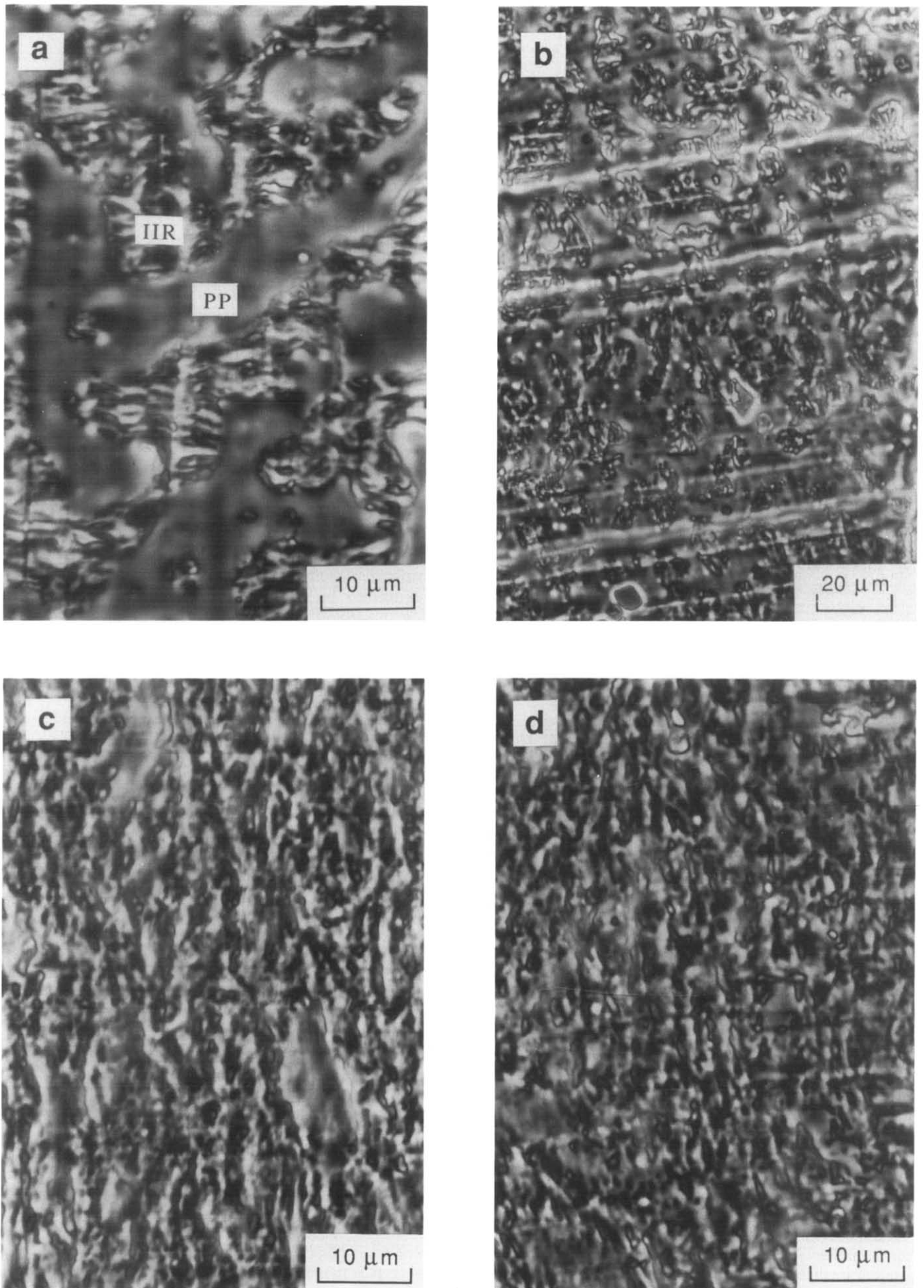


Figure 1 Phase-contrast micrographs of (a) B5-0, (b) B5-0 at lower magnification, (c) B5-4 and (d) B7-4

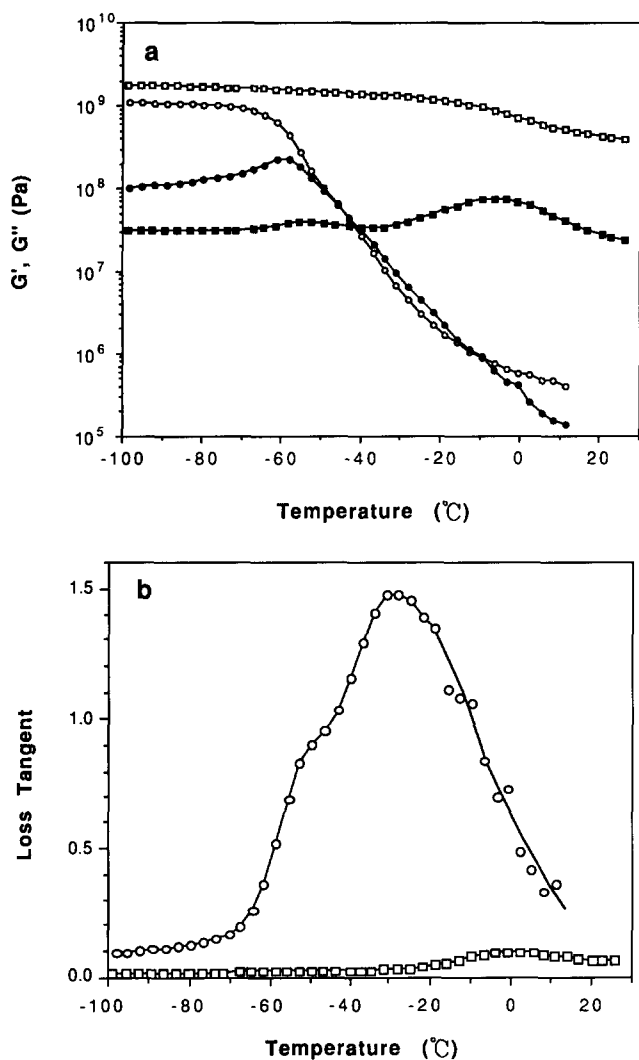


Figure 2 Dynamic mechanical spectra of PP (squares) and I-4 (circles): (a) G' (open symbols) and G'' (filled symbols) and (b) $\tan \delta$

morphology with coalesced IIR domains dispersed in the PP matrix. Although the IIR phase in Figure 1a may appear continuous, observations at lower magnifications (Figure 1b) clearly indicated that IIR is the dispersed phase. The local transverse dimension of the IIR phase zone is of the order of $10\ \mu\text{m}$, whereas the global span of phase connectivity is of the order of $100\ \mu\text{m}$, indicating that the blend is on the verge of dual-phase continuity. The IIR phase zone contains a significant number of occluded PP particles, whereas the PP phase zone is relatively free of IIR occlusion. In the present case, the PP phase is of lower viscosity and elasticity¹⁸. These morphological features are therefore in accord with earlier suggestions that the phase of lower viscosity tends to be the continuous phase¹⁹ and that the phase of lower elasticity tends to be occluded in the other phase²⁰. As for the dynamically vulcanized blends (cf. Figures 1c and 1d), PP appears to be the continuous phase, with comparatively small and irregularly shaped IIR domains dispersed within. Because of field depth effects, however, differences in the volume fraction of the small (i.e. micrometre- and probably some submicrometre-sized) rubber particles are not readily identifiable. Nevertheless, the observation of a continuous PP phase is consistent with the melt processibility of these blends.

Damping behaviour of component polymers

General observations. Dynamic mechanical spectra of PP and a statically vulcanized IIR (namely, I-4) are shown in Figure 2. For PP, maxima in G'' and $\tan \delta$ are at ca. -5 and 0°C , respectively. These values may be related to T_g of PP, as also indicated by the corresponding drop of G' in this temperature range. In addition to T_g , a much weaker transition at ca. -50°C can be identified, which could probably be attributed to the presence of a minor amount of ethylene-propylene copolymer in PP as a common industrial practice.

The IIR vulcanizate exhibits a maximum in G'' near -60°C , above which the G' value decreases clearly with temperature. This is comparable to the reported T_g value¹⁵ of -70°C for polyisobutylene (PIB). Interestingly, the $\tan \delta$ peak is very broad (covering a temperature range of -70 to 10°C) with a maximum at -30°C and a shoulder near -55°C . The low-temperature shoulder corresponds to the T_g of IIR. Doubtlessly, the broad high-temperature maximum is closely related to the well known damping characteristics of IIR. It has been attributed by Dutta and Tripathy⁶ to the stronger drop in the elastic modulus (as compared to the loss modulus) at the higher end of the broad glass transition. This interpretation, however, is purely phenomenological and lacks molecular insights.

In an earlier viscoelasticity study of vulcanized IIR, Sanders and Ferry²¹ observed a similar loss peak at the low-frequency end of the glass transition region, which they termed the 'slow relaxation' process. This delayed 'slow relaxation' process above T_g was later assigned as a liquid-state relaxation (i.e. the 'liquid-liquid transition', T_{ll}) by Boyer²². Results from dilatometry, d.s.c. and torsion braid analysis indicated²³⁻²⁵ that $T_{ll} \approx -20^{\circ}\text{C}$ for PIB, in agreement with the position of the $\tan \delta$ maximum here. The exact molecular origin of T_{ll} is not clear at the present time. Boyer²² proposed that T_{ll} is related to the disruption of short-range order (or local packing) with increasing temperature.

Statically cured IIR of various curative levels. Dynamic mechanical spectra (measured with a slightly higher maximum strain of 0.2% for improved signal-to-noise level) of statically vulcanized IIR at different curative loadings are shown in Figure 3. It may be observed that T_g (i.e. the 'knee' of the G' curve, the maximum of the G'' curve, or the low-temperature shoulder of the broad $\tan \delta$ peak) in the vicinity of -60°C is shifted to a slightly higher temperature upon the first addition of curative but the effect levels off at higher curative loadings. Above T_g the G' and G'' curves are elevated (or shifted to the high-temperature side); the effects of curative loading on the extent of the shift are similar to the case of T_g . As a direct result of shifts in G' and G'' curves, the broad $\tan \delta$ peak has shifted from ca. -40 to ca. -30°C .

Variations of the gel fraction (ϕ_{gel}) and the bulk crosslinking density (ν_{bulk}) of the IIR vulcanizates with curative loading are given in Table 2. At a relatively low curative level of 2.5 phr, ϕ_{gel} and ν_{bulk} in I-1 are already respectable. Further increases in the curative loading resulted in only minor increases in ϕ_{gel} and ν_{bulk} . These are parallel to the observations in the dynamic mechanical behaviour of IIR vulcanizates just described. Crosslinking has been shown^{26,27} to affect T_i ; the transition temperature increases with the extent of crosslinking if the crosslinking density is below a certain threshold limit (ν_{th}). In addition,

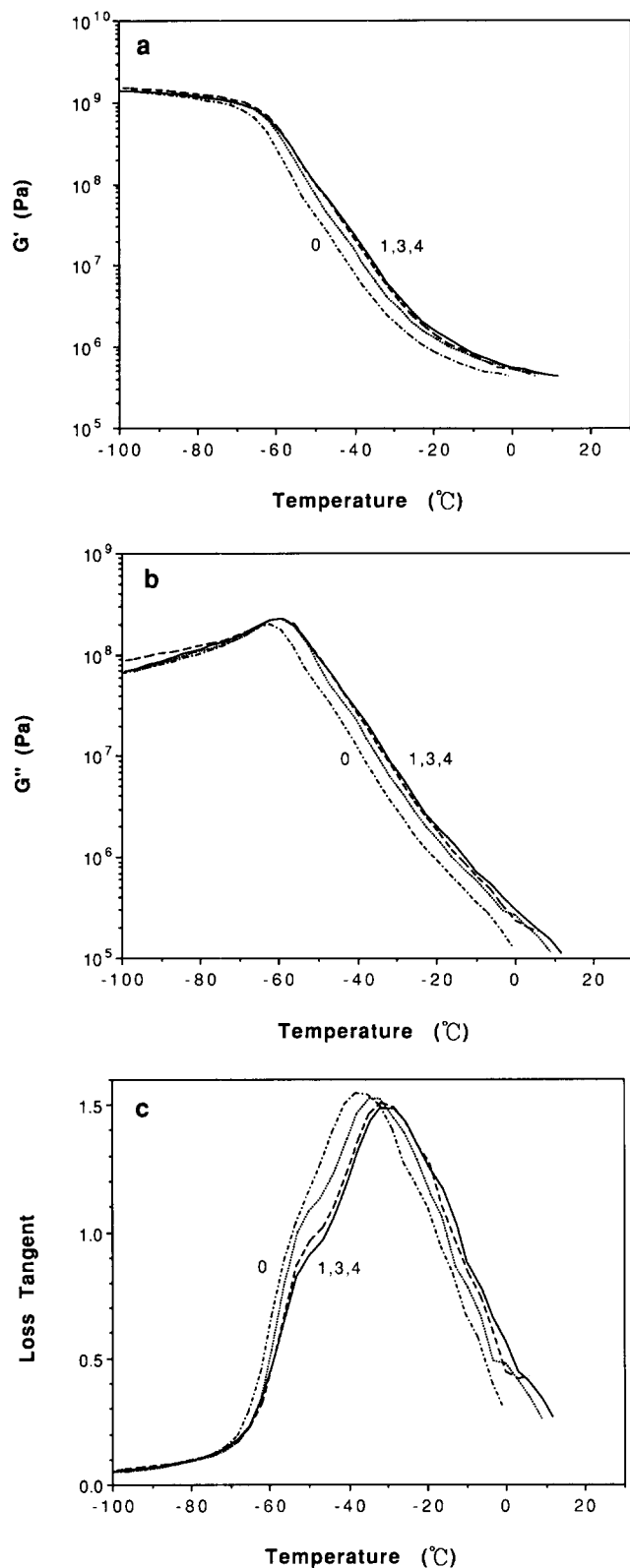


Figure 3 Variation of (a) G' , (b) G'' and (c) $\tan \delta$ of IIR with curative level: curves 0, 1, 3 and 4 correspond to I-0, I-1, I-3 and I-4, respectively

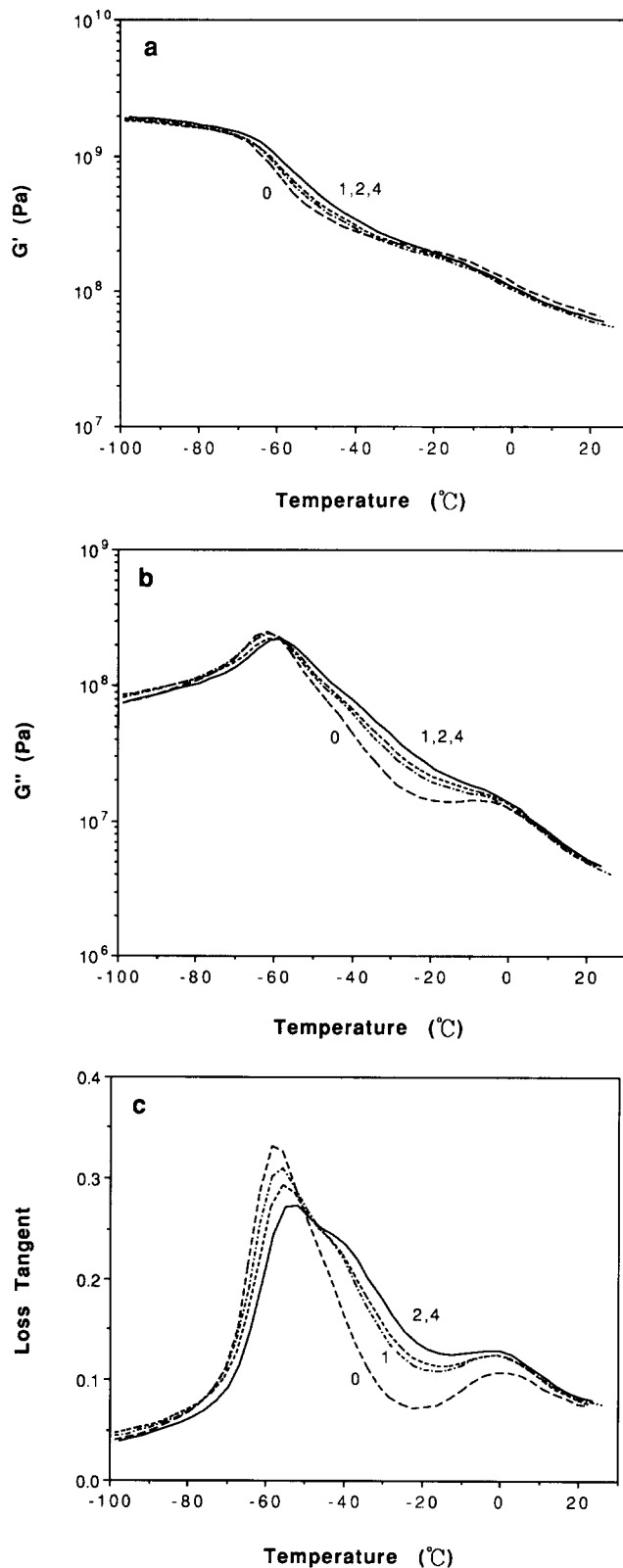


Figure 4 Variation of (a) G' , (b) G'' and (c) $\tan \delta$ with curative level at a fixed IIR/PP ratio: curves 0, 1, 2 and 4 correspond to B5-0, B5-1, B5-2 and B5-4, respectively

as the crosslinking density increases, the intensity of the liquid-liquid transition tends to decrease slightly; above ν_{th} , the intensity of T_{ll} drops dramatically and virtually disappears. This threshold limit corresponds^{26,27} to approximately 200 backbone bonds between crosslinks. The relatively narrow crosslinking density range of $13 \pm 2 \text{ mol m}^{-3}$ (which corresponds to ca. 700 backbone

bonds between crosslinks) in the present vulcanizates is significantly lower than the expected ν_{th} of ca. 45 mol m^{-3} . Therefore, both the shift towards higher temperatures with increasing ν_{bulk} and the relatively constant peak intensity of the strong $\tan \delta$ maximum appear consistent with the assignment of T_{ll} .

Dynamically cured blends of various curative levels

General observations. Dynamic mechanical spectra of dynamically cured blends with a fixed IIR/PP ratio (50/50 w/w) but different curative loadings (i.e. 0–10 phr with respect to IIR) are shown in *Figure 4*. Consistent with the microscopic observations, these blends appear heterogeneous, showing typical two- T_g (at ca. -60 and -5°C , respectively) behaviour in the G' and G'' curves. With increasing curative loading, the G'' curve is elevated at temperatures between the two T_g values. A similar observation may be made for G' , but the effect is apparent only at the low-temperature range. The T_g of the IIR phase increases slightly with the curative loading whereas that of the PP phase remains essentially constant.

The behaviour of the $\tan \delta$ curve is more interesting. The first thing to note is that the intensity of the T_{11} maximum of IIR is strongly suppressed (cf. *Figure 3*, note also the difference in the ordinate scale), appearing here as a shoulder overlapping with T_g of the IIR phase. This effect is most apparent in the absence of the curative where the T_{11} peak almost merges entirely with the T_g peak. With increasing curative level, both the T_g peak and especially the T_{11} shoulder shift towards higher temperatures, rendering the latter more clearly discernible. On the other hand, the T_g peak of the PP phase (at ca. 0°C) appears to shift slightly towards lower temperatures and increase significantly in intensity. A parallel d.s.c. analysis indicated that the crystallinity of the PP phase in these blends is essentially constant (i.e. $25 \pm 1\%$), which rules out the possibility of increased $\tan \delta$ peak intensity due to decreased crystallinity. This increase in intensity and the minor shift in the peak position are more likely due to the overlapping effect from the broad T_{11} peak of the IIR phase.

Crosslinking in the IIR phase. Network characteristics of the IIR phase in these blends are given in *Table 3*. Similar to statically cured IIR, ϕ_{gel} values at relatively low curative levels of 2.5 and 5 phr are already respectable, and further increases in the curative loading result in comparatively minor increases in ϕ_{gel} . Similar observations may be made on v_{bulk} (or v_{gel}). Interestingly, the crosslinking density of the IIR phase in blends of higher curative levels (i.e. B5-2 to B5-4) are significantly higher than that of the statically cured IIR counterparts. The reason for this behaviour is not clear at the present time. In view of the low unsaturation level of IIR, crosslinking induced by thermomechanical degradation²⁸ is unlikely to occur to a significant extent.

Table 3 Characteristics of the IIR phase in dynamically cured blends at a fixed composition (IIR/PP = 50/50 w/w) but different curative loadings^a

Sample code	ϕ_{gel}^b	v_{gel}^c (mol m^{-3})	$v_{\text{bulk, calc}}^d$ (mol m^{-3})
B5-1	0.82	15	12
B5-2	0.90	26	23
B5-3	0.92	35	32
B5-4	0.93	34	32

^a Cf. *Table 1* for sample designations

^b Soxhlet extraction in boiling xylene

^c Equilibrium swelling of the xylene-insolubles in cyclohexane at room temperature

^d Calculated according to equation (2)

Thermal misfit between PP and IIR. In the present blends, significant thermal stresses exist due to the mismatch in the volumetric thermal expansion coefficients ($\alpha_{\text{PP}} \approx 3 \times 10^{-4} \text{ }^\circ\text{C}^{-1}$ and $\alpha_{\text{IIR}} \approx 6 \times 10^{-4} \text{ }^\circ\text{C}^{-1}$)¹⁵. The thermal stress (σ) within a rubber particle may be estimated according to²⁹:

$$\sigma = \frac{K_d(\alpha_m - \alpha_d)\Delta T}{1 + (K_d/K_m\phi_m)[(1 + \mu_m)/2(1 - 2\mu_m) + \phi_d]} \quad (3)$$

where ΔT is the decrease in temperature from the stress-free state, K is the bulk modulus, μ is the Poisson ratio, ϕ is the volume fraction, and subscripts m and d denote respectively the matrix and the dispersed phases. Taking¹⁵ $K_{\text{PP}} = 2.0 \text{ GPa}$, $K_{\text{IIR}} = 3.5 \text{ GPa}$, $\mu_{\text{PP}} = 0.4$, neglecting the density difference, and assuming that the PP matrix solidifies at ca. 110°C ³⁰, equation (3) indicated that $\sigma \approx 10 \text{ MPa}$ (i.e. a dilatational stress or a negative pressure) within the IIR phase of the present B5 blends at ca. -30°C .

Effects of crosslinking and thermal misfit. It has been established²² that T_{11} is very sensitive to pressure. The intensity as well as the position of T_{11} increases with pressure. The dramatic suppression of the T_{11} peak intensity in these blends is therefore attributable to the presence of a significant negative pressure in the IIR phase. The pressure coefficients for T_g and T_{11} of IIR are²³ $dT_g/dP = 0.24^\circ\text{C MPa}^{-1}$ and $dT_{11}/dP = -1.2^\circ\text{C MPa}^{-1}$. Therefore, a thermal stress of ca. 10 MPa should result in a -2°C shift in T_g and a -12°C shift in T_{11} , in good agreement with the observed merge of T_g and T_{11} peaks in *Figure 4c* for the B5-0 blend. On the other hand, the crosslinking of IIR tends to increase T_{11} . This results in the gradual separation of T_g and T_{11} with increasing curative level in dynamically cured B5 blends. It should be noted that, even though the IIR phase in B5 blends is comparatively higher in crosslinking density, the T_{11} peak position is still lower than in the unblended IIR counterpart. It may therefore be concluded that the thermal stress plays the dominant role here. Not only the position but also the intensity of the T_{11} peak is strongly suppressed; the crosslinking of IIR compensates part of the former effect but none of the latter.

Dynamically cured blends of various IIR/PP ratios

General observations. Dynamic mechanical spectra of dynamically cured blends with a fixed curative level (10 phr) but different IIR contents are shown in *Figure 5*. The G' curves (cf. *Figure 5a*) exhibit a clear break at ca. -60°C , which corresponds to the T_g of IIR; another break, barely discernible, is located in the vicinity of -5°C , which corresponds to the T_g of PP. At the high-temperature end, G' curves are nearly equally spaced, with blends of higher IIR contents lying lower. The G' curves approach one another with decreasing temperature and finally merge into a single curve below T_g of the IIR phase. Similar to the case of G' , the G'' curves (cf. *Figure 5b*) also exhibit a clear maximum at ca. -60°C and a weak shoulder at ca. -5°C , corresponding to the T_g values of the two phases. At low temperatures (i.e. below -40°C), blends of higher IIR contents tend to have higher G'' values; the trend is reversed in the high-temperature range, where blends of low IIR contents tend to have higher G'' values.

As for the $\tan \delta$ curves (cf. *Figure 5c*), three peaks may be identified: the high-temperature peak at ca. 0°C

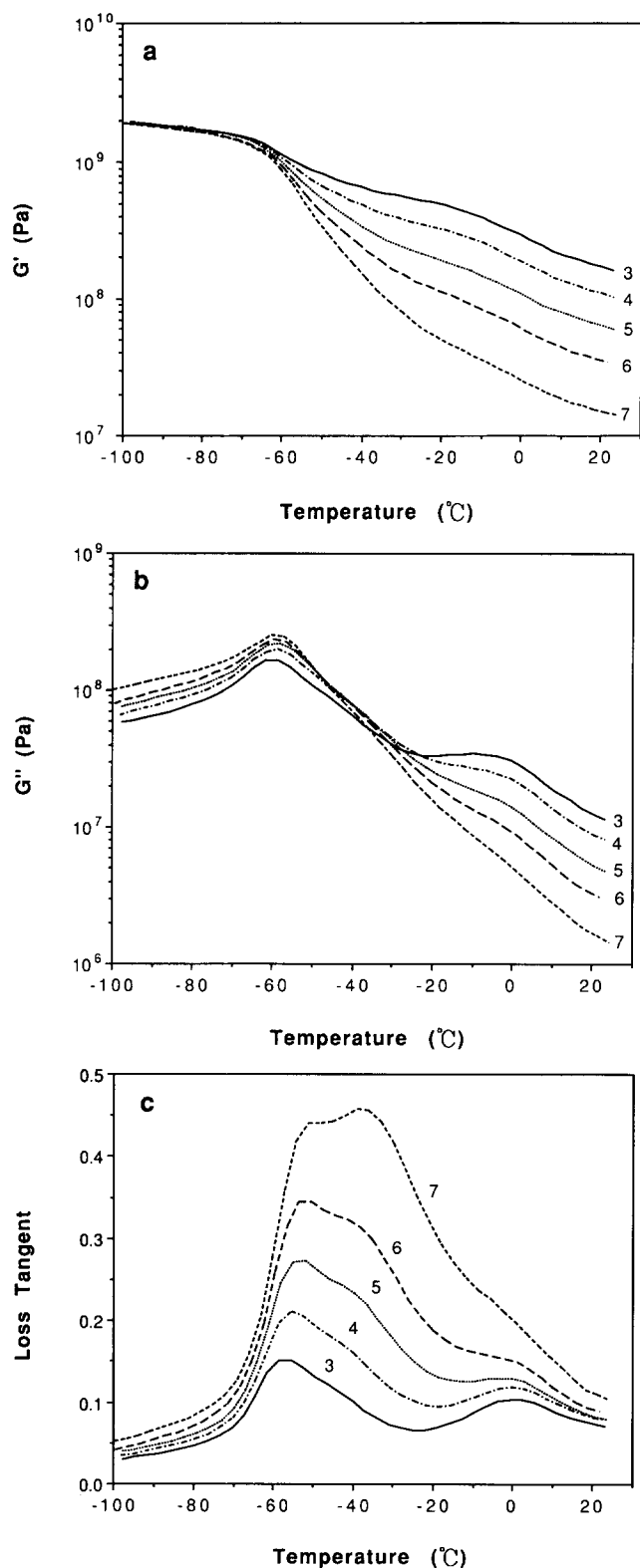


Figure 5 Variation of (a) G' , (b) G'' and (c) $\tan \delta$ with blend composition at a fixed curative level: curves 3 to 7 represent B3-4 to B7-4, respectively

corresponds to T_g of PP, whereas the low-temperature peaks at ca. -60 and -40°C correspond to T_g and T_{11} of the IIR phase. The intensity of each of the three peaks increases with IIR content. The position of the T_g peak of PP is insensitive to the presence of IIR, whereas T_g and T_{11} peaks of IIR tend to shift towards higher temperatures with increasing IIR content. The relative intensity of the T_{11} peak (as compared to that of the T_g peak) of the IIR phase also increases with IIR content.

Table 4 Characteristics of the IIR phase in dynamically cured blends of various IIR/PP ratios^a but a fixed curative level of 10 phr

Sample code	ϕ_{gel}^b	v_{gel}^c (mol m ⁻³)	$v_{\text{bulk,calc}}^d$ (mol m ⁻³)
B3-4	0.84	26	22
B4-4	0.85	28	24
B5-4	0.93	34	32
B6-4	0.95	36	34
B7-4	0.90	41	37

^a Cf. Table 1 for sample designations

^b Soxhlet extraction in boiling xylene

^c Equilibrium swelling of the material remaining after Soxhlet extraction in cyclohexane at room temperature

^d Calculated according to equation (2)

Effects of crosslinking and thermal misfit. Network characteristics of the IIR phase in these blends are given in Table 4. Similar to the B5 series discussed above, the crosslinking density of the IIR phase in these blends is higher than in the unblended, statically cured counterpart (i.e. I-4). In addition, ϕ_{gel} and v_{bulk} increase with IIR content. This is again unexpected in the present case of fixed curative loading. One may suggest that curative migration might play a role here; however, the fact that these dynamically cured blends have higher v_{bulk} values than the unblended IIR vulcanizates indicates that this effect should not be very significant. As addressed in the discussion on the B5 series, thermomechanically induced crosslinking should not be significant either. The peculiar behaviour of the crosslinking in the IIR phase awaits further investigation.

Calculations based on equation (3) indicated significant thermal stresses in the IIR phase at ca. -30°C . The misfit stress increases with decreasing IIR content, ranging from 14 MPa for B3-4 to 6 MPa for B7-4. These would result in a -3°C shift in T_g and a -16°C shift in T_{11} for B3-4 or a -1°C shift in T_g and a -7°C shift in T_{11} for B7-4. However, the increasing crosslinking density with increasing IIR content counterbalances partly the stress effect on T_{11} . As a result, somewhat parallel shifts in T_g and T_{11} are observed. On the other hand, the suppressive effect of misfit stress on the intensity of the T_{11} peak remains undisturbed, resulting in decreased T_{11} peak height (as compared to the intensity of the corresponding T_g peak) in these blends, especially when the IIR content is low.

CONCLUSIONS

In summary, the damping characteristics of the dynamically cured IIR/PP blends in the present temperature range of -100 to 25°C exhibited interesting dependence on both the blend composition and the curative level. This can be explained in terms of the dependence of a liquid-state relaxation (T_{11}) of IIR on the stress state and the extent of crosslinking. The continuous PP matrix, which provides plastic-like processibility to the present blends, may result in a significant thermal misfit stress in the IIR phase, which in turn suppresses the intensity as well as the position of T_{11} . The crosslinking of IIR counterbalances part of the latter effect but none of the former.

These observations imply that the combination of a low PP level (just enough to maintain its phase

continuity) and a reasonably high extent of IIR cross-linking is advantageous in the damping performance of dynamically cured IIR/PP blends. In this optimal case, the prominent T_{11} peak may overlap extensively with the T_g peaks of IIR and PP, resulting in a broad temperature range (from ca. -60°C to room temperature) of significant damping capability.

ACKNOWLEDGEMENTS

Thanks are due to Mr Ming-Sung Chang at NMRD of CSC for his help in sample preparation. Thanks should also be extended to Prof. P. W. Kao at IMSE of NSYSU for enlightening discussions on thermal misfit stress.

REFERENCES

- 1 Brydson, J. A. 'Rubbery Materials and Their Properties', Elsevier, London, 1988, Ch. 8
- 2 Smith, W. C. in 'Vulcanization of Elastomers' (Eds. G. Alliger and I. J. Sjothun), Krieger, Huntington, NY, 1964
- 3 Lattimer, R. P., Kinsey, R. A., Layer, R. W. and Rhee, C. K. *Rubber Chem. Technol.* 1989, **62**, 107
- 4 Capps, R. N. *Rubber Chem. Technol.* 1986, **59**, 103
- 5 Capps, R. N. and Burns, J. J. *Non-Cryst. Solids* 1991, **131-133**, 877
- 6 Dutta, N. K. and Tripathy, D. K. *Polym. Degrad. Stab.* 1990, **30**, 231
- 7 Kresge, E. N. in 'Polymer Blends' (Eds. D. R. Paul and S. Newman), Academic Press, New York, 1978, Ch. 20
- 8 Coran, A. Y. in 'Thermoplastic Elastomers' (Eds. N. R. Legge, G. Holden and H. E. Schroeder), Hanser, Munich, 1987, Ch. 7
- 9 Rader, C. P. in 'Handbook of Thermoplastic Elastomers', 2nd Edn (Eds. B. M. Walker and C. P. Rader), Van Nostrand Reinhold, New York, 1988, Ch. 4
- 10 Legge, N. R. *Rubber Chem. Technol.* 1989, **62**, 529
- 11 Rader, C. P. and Abdou-Sabet, S. in 'Thermoplastic Elastomers from Rubber-Plastic Blends' (Eds. S. K. De and A. K. Bhowmick), Ellis Horwood, New York, 1990, Ch. 6
- 12 Puydak, R. and Hazelton, D. Proc. 47th Annu. Tech. Conf., Soc. Plast. Eng. 1988, p. 1731
- 13 Liao, F. S., Hsu, T. J. and Su, A. C. *J. Appl. Polym. Sci.* 1993, **48**, 1801
- 14 Kerwin, E. M., Jr *J. Acoust. Soc. Am.* 1959, **31**, 952
- 15 'Polymer Handbook' (Eds. J. Brandrup and E. H. Immergut), Wiley, New York, 1989
- 16 Flory, P. J. 'Principles of Polymer Chemistry', Cornell University Press, Ithaca, NY, 1953, Ch. 13
- 17 Sheehan, C. J. and Bisio, A. L. *Rubber Chem. Technol.* 1966, **39**, 149
- 18 Liao, F. S., Su, A. C. and Hsu, T. J., unpublished results
- 19 Paul, D. R. and Barlow, J. W. *J. Macromol. Sci. (C)* 1980, **18**, 109
- 20 van Oene, H. J. *Colloid Interface Sci.* 1972, **40**, 440
- 21 Sanders, J. F. and Ferry, J. D. *Macromolecules* 1975, **7**, 681
- 22 Boyer, R. F. in 'Order in the Amorphous State of Polymers' (Eds. S. E. Keinath, R. L. Miller and J. K. Rieke), Plenum, New York, 1987, p. 135
- 23 Boyer, R. F. *Macromolecules* 1981, **14**, 376
- 24 Keinath, S. E. and Boyer, R. F. *J. Appl. Polym. Sci.* 1983, **28**, 2105
- 25 Boyer, R. F. *J. Appl. Polym. Sci.* 1986, **32**, 4075
- 26 Boyer, R. F. *Rubber Chem. Technol.* 1963, **36**, 1303
- 27 Enns, J. B. and Boyer, R. F. in 'Order in the Amorphous State of Polymers' (Eds. S. E. Keinath, R. L. Miller and J. K. Rieke), Plenum, New York, 1987, p. 221
- 28 Ho, R. M., Wu, C. H. and Su, A. C. *Polym. Eng. Sci.* 1990, **30**, 511
- 29 Boyce, M. E., Argon, A. S. and Parks, D. M. *Polymer* 1987, **28**, 1680
- 30 Chen, Y. J. and Su, A. C., unpublished results